Supplementary Information

Plasmon-Enhanced Two-Photon-Induced Isomerization for Highly-Localized Light-Based Actuation of Inorganic/Organic Interfaces

*Chang-Keun Lim, Xin Li, Yue Li, Kurt L. M. Drew, J. Pablo Palafox-Hernandez, Zhenghua Tang, Alexander Baev, Andrey N. Kuzmin, Marc R. Knecht, Tiffany R. Walsh, Mark T. Swihart, Hans Ågren, and Paras N. Prasad**

List of contents for supporting information

switching, samples were illuminated with monochromatic 350 nm light from a Xe lamp for 30 min, and then a focused 880 nm femtosecond pulsed laser was used to illuminate a small focal volume within the cuvette.

Fig. S6 Changes in absorbance spectra upon attempted nonlinear *trans* to *cis* photoswitching of (a) MAM-CAuBP1 and (b) AuBP1C-MAM on Ag NPs. The colloidal dispersion was illuminated with a femtosecond pulsed 700 nm laser.

Fig. S7 Excitation power dependence of isomerization of *cis*-AuBP1C-MAM on Ag NPs under pulsed laser illumination at 880 nm.

Fig. S8. Changes in absorbance spectra of *trans*-MAM-CAuBP1 capped Ag NPs upon focused (a) 700, (b) 800, (c) 900 and (d) 1000 nm femtosecond pulsed laser illumination for 1 h.

Fig. S9 (a) Suggested mechanism of isomerization of azobenzene derivative. (b) Schematic representation of 1- and 2-photon induced isomerization upon 350 and 700 nm excitations. SPA and TPA signify single photon absorption and two photon absorption respectively.

Fig. S10 Thermal imaging results for solutions of AF-350 two-photon dye (a) and silver nanoparticles (b) in a mixture of DMSO and water (4:1) under femtosecond pulsed IR laser illumination (818 nm) and corresponding intensity profiles (c) along lines shown in (a) and (b). Pictures were obtained by subtracting of confocal images in Stokes (excited at 543 nm) and anti-Stokes (excited at 633 nm) modes of the area, where the stationary IR beam was focused in the solutions. Imaging area 35x35 μm^2. Black profile corresponds to image (a) and red curve – to image (b).

Fig. S11 Frontier molecular orbitals of *trans*- and *cis*-azobenzene.

Fig. S12 Cross-sectional view of the distribution of electric field strength for Ag nanoparticles with different diameters placed in a uniform external electric field of 0.5 V nm^{-1}.

3. Supplementary Tables

Table S1. Computed photon energies and TPA cross sections for trans-azobenzene.

Table S2. Computed photon energies and TPA cross sections for cis-azobenzene.

Table S3. Calculated dipole moment and transition dipole moment (in a.u.) for ground state and low-lying excited states of *trans*-azobenzene.

Table S4. Calculated dipole moment and transition dipole moment (in a.u.) for ground state and low-lying excited states of *cis*-azobenzene.

Table S5. Calculated two-photon absorption cross-section (in GM) for the most probable conformations of *trans*-azobenzene.

Table S6. Calculated two-photon absorption cross-section (in GM) for the most probable conformations of *cis*-azobenzene.

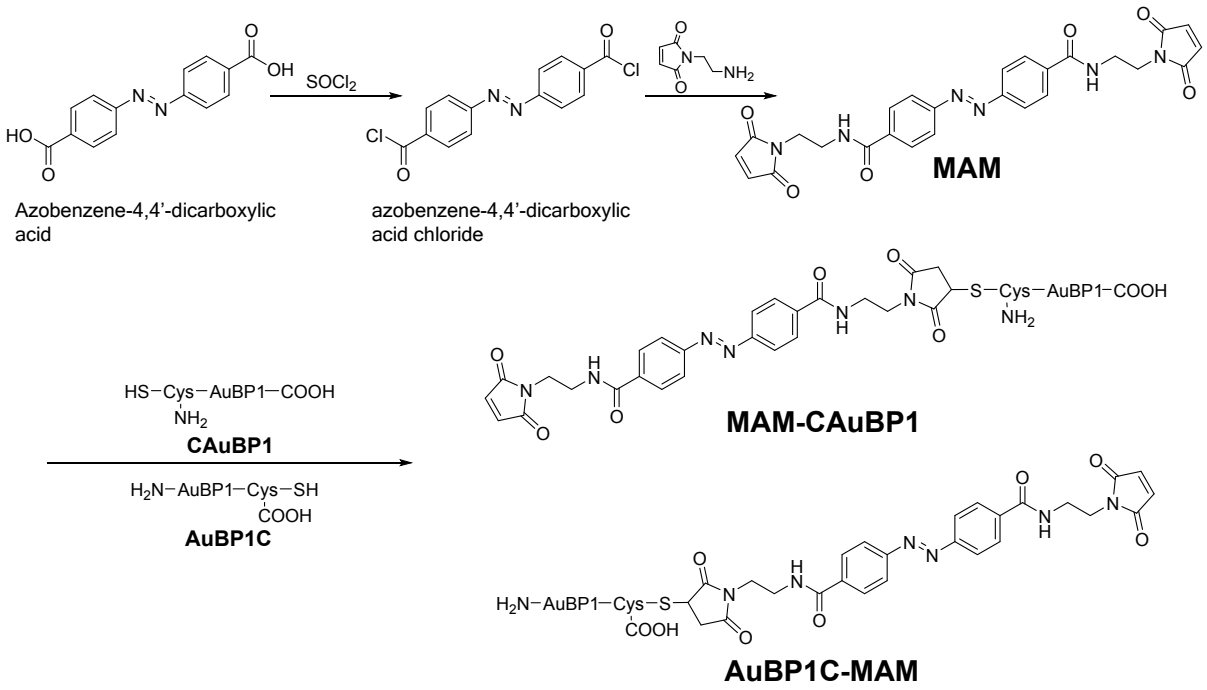

Scheme S1. Synthetic route for producing MAM-CAuBP1 and AuBP1C-MAM.

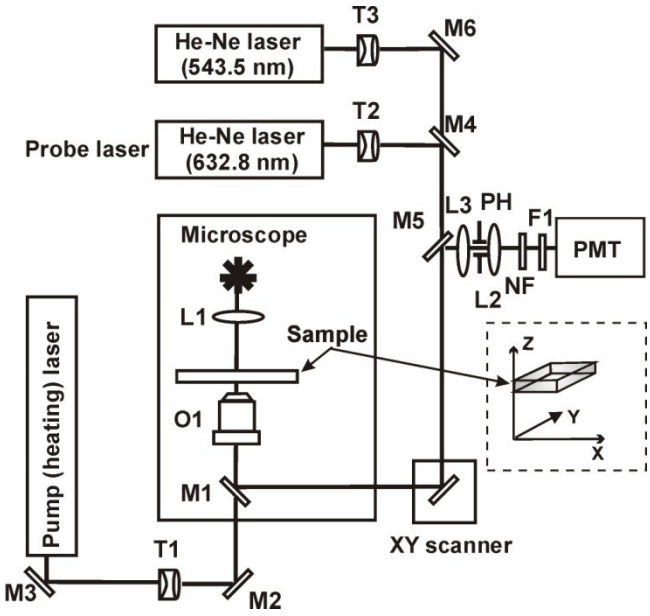

Fig. S1 Experimental setup for thermal imaging; L- lens, M- mirror, T- telescope, PH- pinhole, F- filter, NF – notch filter.

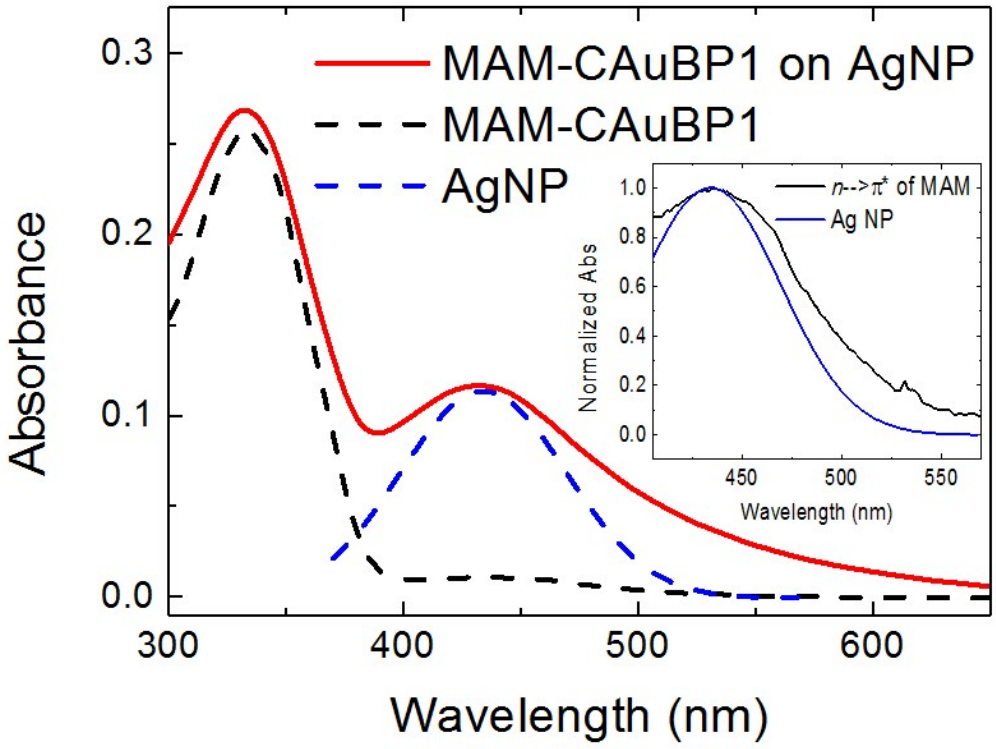

Fig. S2 Spectral deconvolution of MAM-CAuBP1-capped Ag NPs. The spectra were deconvoluted as the sum of an absorption band of the peptide/MAM conjugate and plasmon band of the Ag NPs. Insets show normalized spectra of the $n \rightarrow \pi^*$ transition band of the MAM and the plasmon band of Ag NPs.

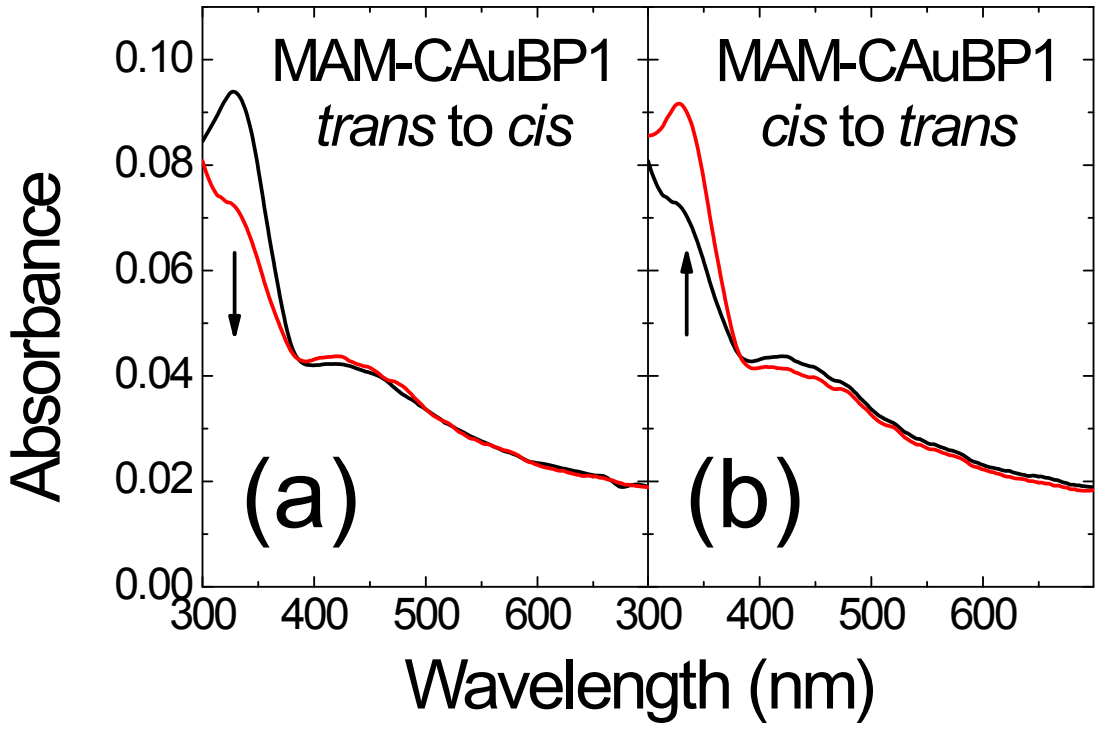

Fig. S3 Changes in absorbance spectra upon linear photoswitching of MAM-CAuBP1 capped Ag NPs. 350 nm and 440 nm monochromatic light from a xenon lamp was used to induce the (a) *trans* to *cis* and (b) *cis* to *trans* switching, respectively.

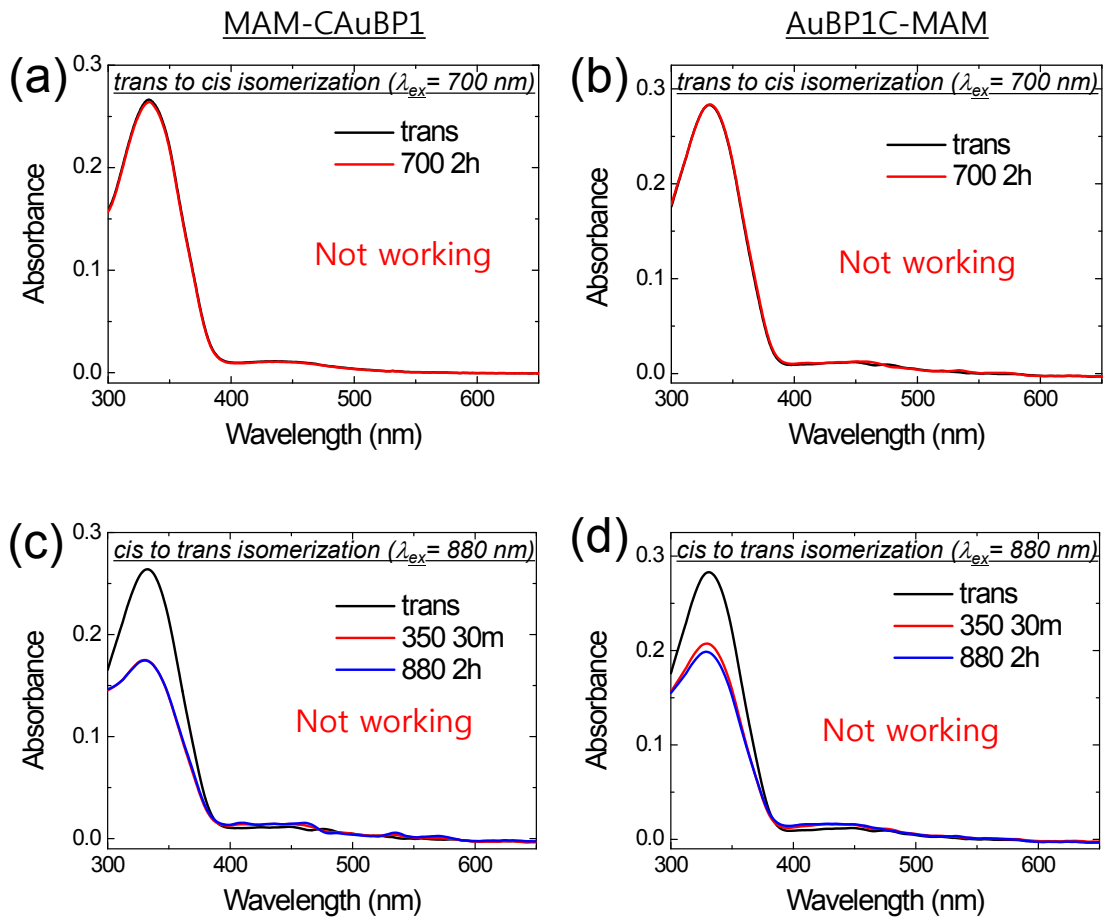

Fig. S4 Changes in absorbance spectra upon nonlinear photoswitching of MAM-CAuBP1 (a and c) and AuBP1C-MAM (b and d) in solution. The solution, without Ag NPs was illuminated by focused 700 nm and 880 nm lasers in an attempt to trigger the *trans* to *cis* (a and b) and *cis* to *trans* (c and d) switching, respectively. Before the *cis* to *trans* switching, the *trans* isomers were converted to *cis* isomers by illumination with monochromatic 350 nm light from a Xe lamp for 30 min.

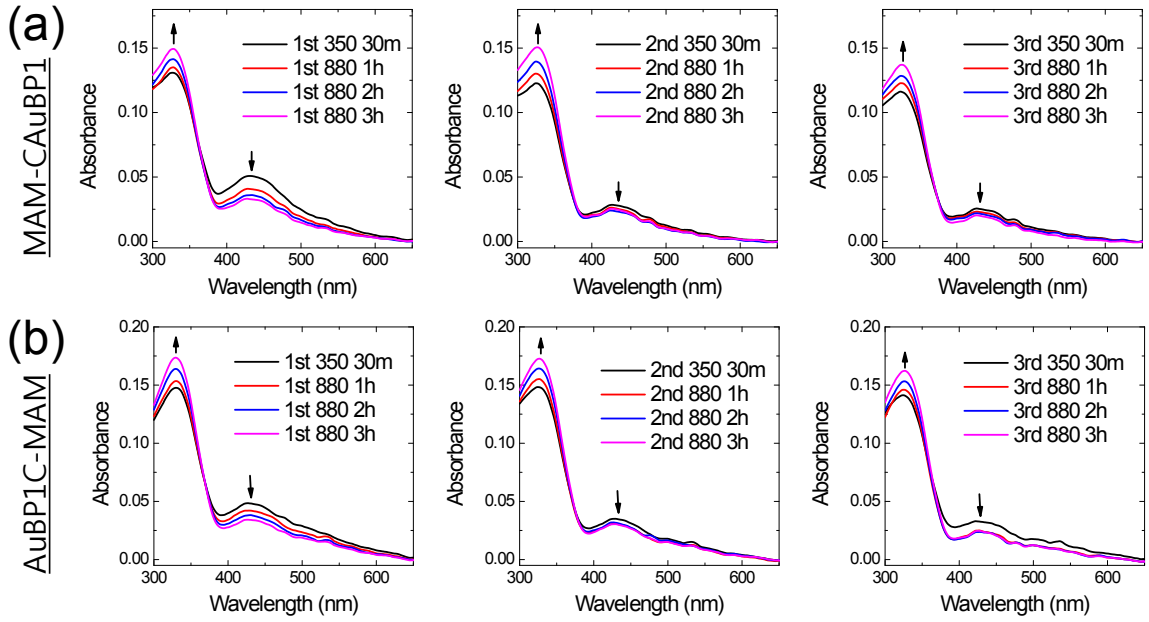

Fig. S5 Changes in absorbance spectra upon nonlinear *cis* to *trans* photoswitching of (a) MAM-CAuBP1 and (b) AuBP1C-MAM on Ag NPs. The switching was repeated three times. Before each switching, samples were illuminated with monochromatic 350 nm light from a Xe lamp for 30 min, and then a focused 880 nm femtosecond pulsed laser was used to illuminate a small focal volume within the cuvette.

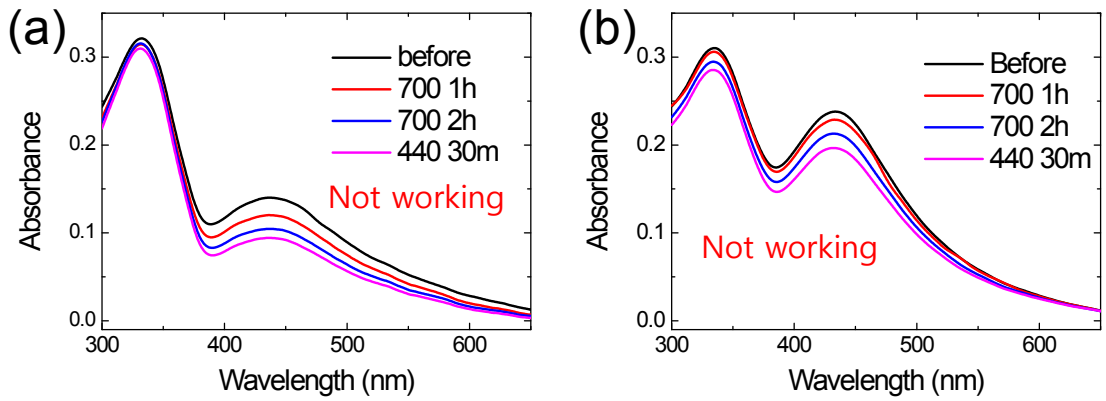

Fig. S6 Changes in absorbance spectra upon attempted nonlinear *trans* to *cis* photoswitching of (a) MAM-CAuBP1 and (b) AuBP1C-MAM on Ag NPs. The colloidal dispersion was illuminated with a femtosecond pulsed 700 nm laser.

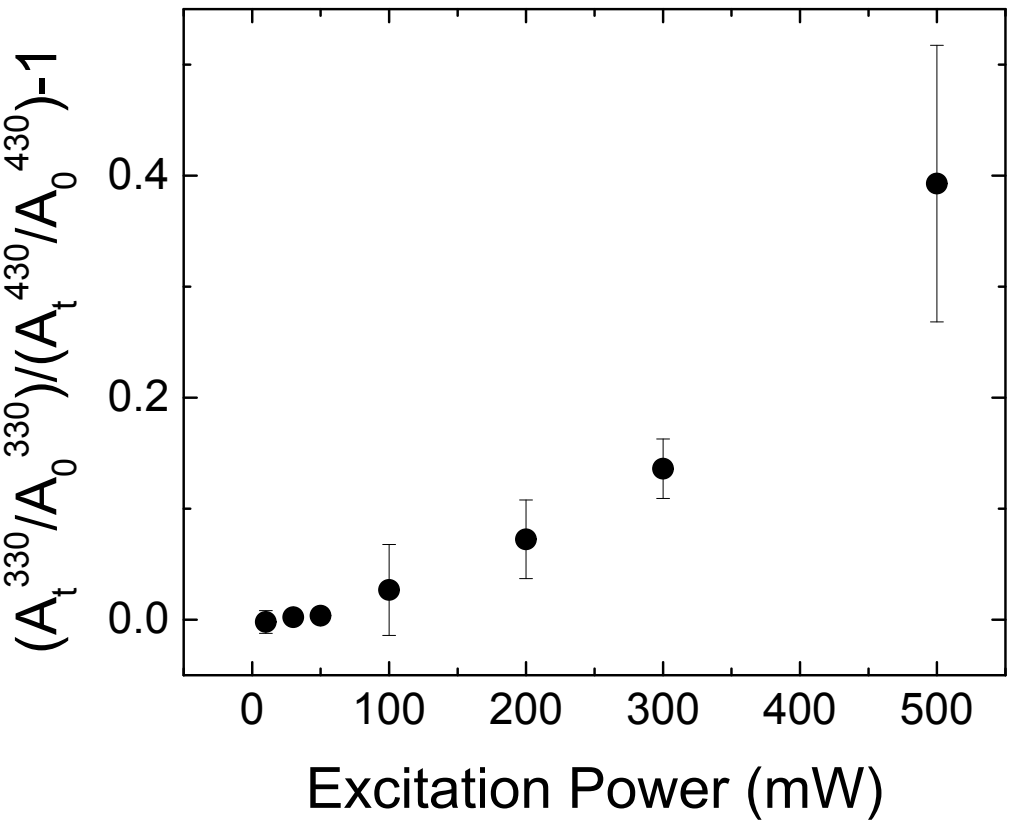

Fig. S7 Excitation power dependency of isomerization of *cis*-AuBP1C-MAM on Ag NPs under pulse laser illumination at 880 nm for 1h.

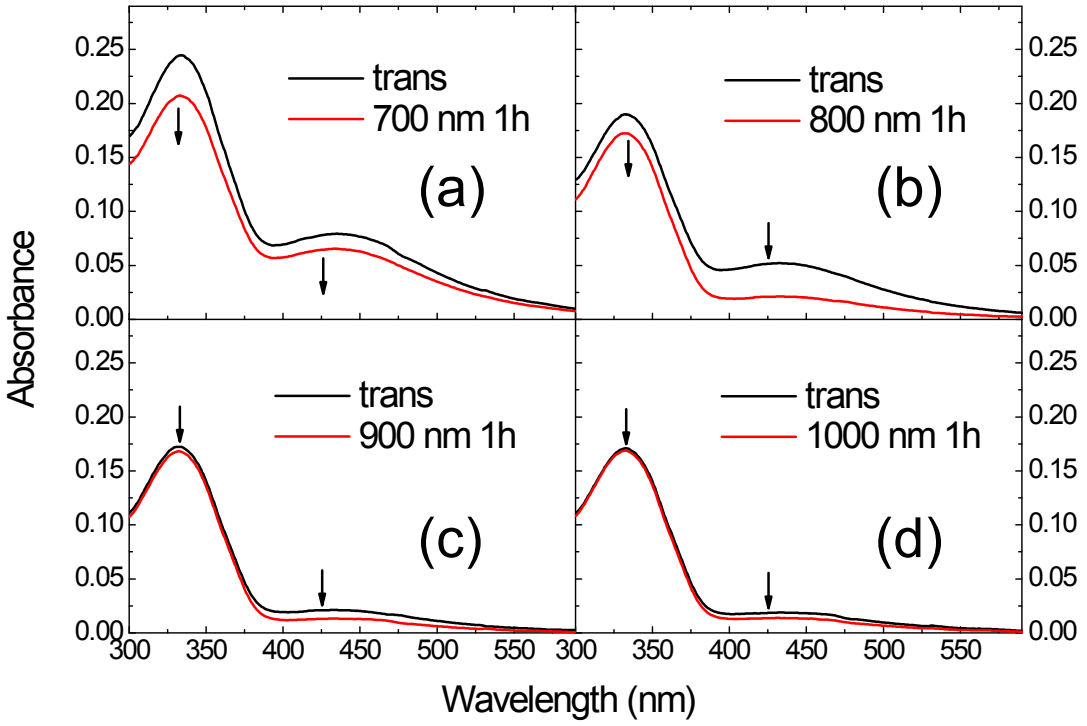

Fig. S8 Changes in absorbance spectra of *trans*-MAM-CAuBP1 capped Ag NPs upon focused (a) 700, (b) 800, (c) 900 and (d) 1000 nm femtosecond pulsed laser illumination for 1 h.

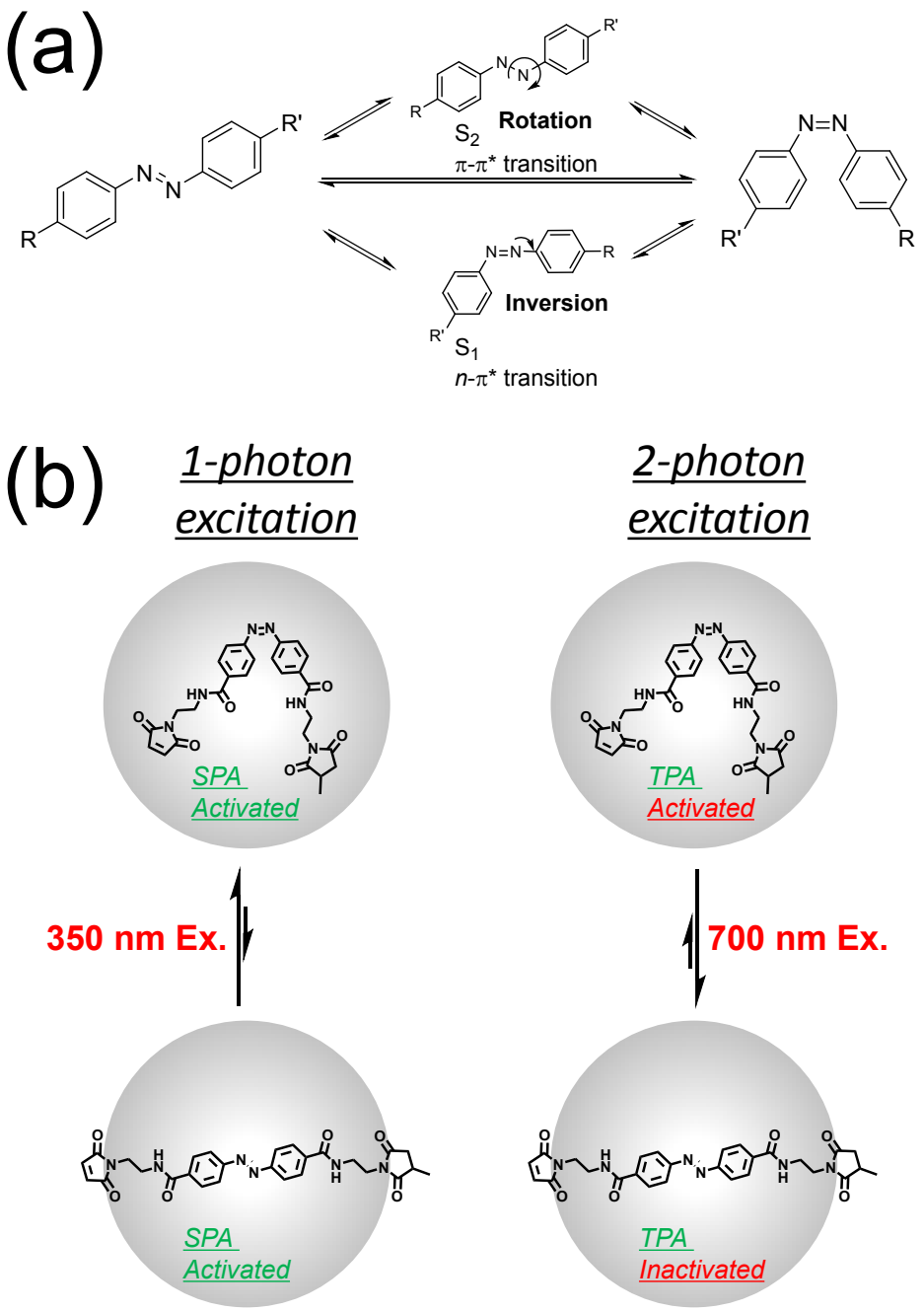

Fig. S9 (a) Suggested mechanism of isomerization of azobenzene derivative. (b) Schematic representation of 1- and 2-photon induced isomerization upon 350 and 700 nm excitations. SPA andTPA signify single-photon absorption and two-photon absorption respectively.

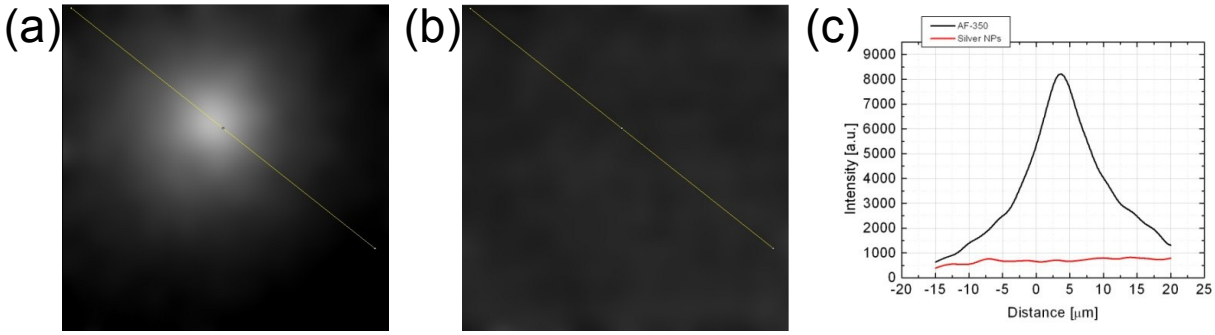

Fig. S10 Thermal imaging results for solutions of AF-350 two-photon dye (a) and silver nanoparticles (b) in a mixture of DMSO and water (4:1) under picosecond pulsed IR laser illumination (818 nm) and corresponding intensity profiles (c) along lines shown in (a) and (b). Pictures were obtained by subtracting of confocal images in Stokes (excited at 543 nm) and anti-Stokes (excited at 633 nm) modes of the area, where the stationary IR beam was focused in the solutions. Imaging area 35x35 μm^2. Black profile corresponds to image (a) and red curve – to image (b).

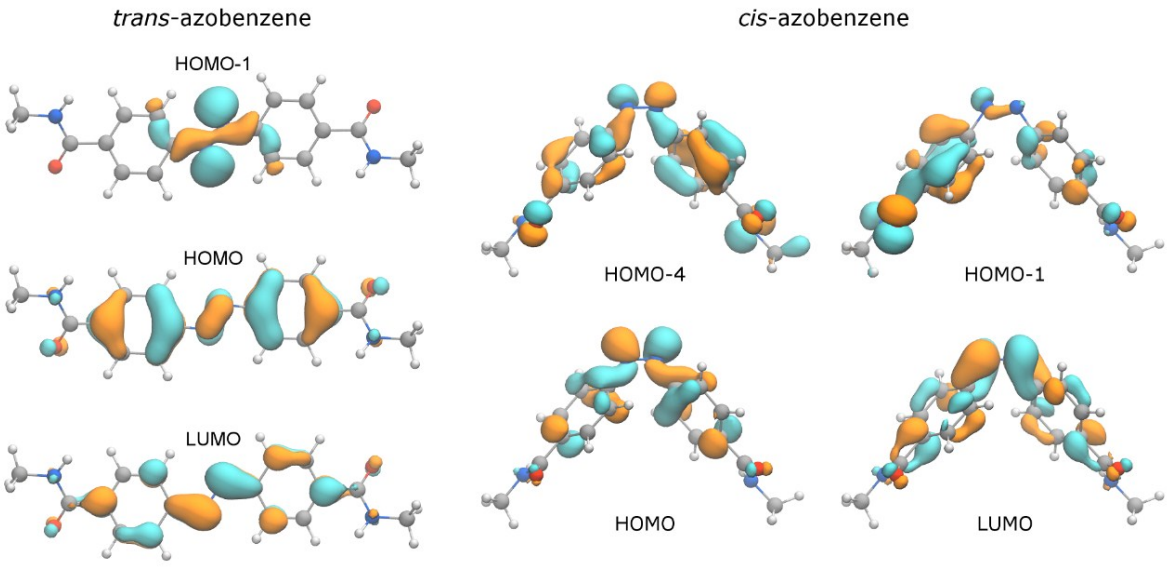

Fig. S11 Frontier molecular orbitals of *trans*- and *cis*-azobenzene.

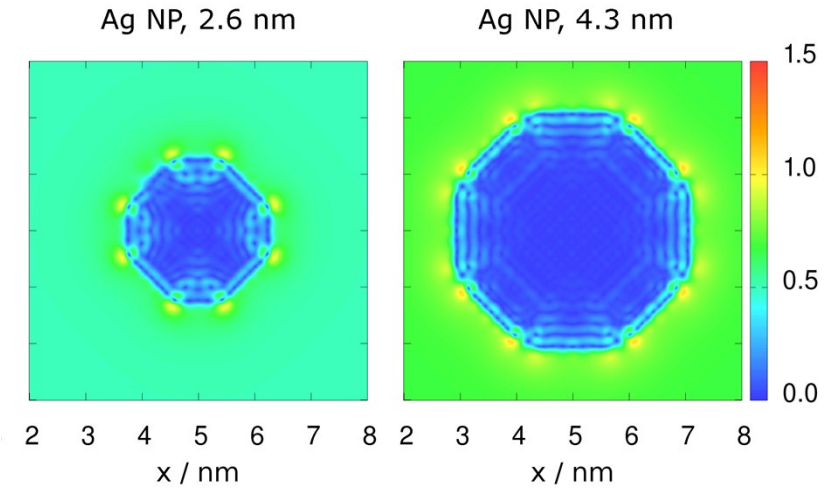

Fig. S12 Cross-sectional view of the distribution of electric field strength for Ag nanoparticles with different diameters placed in a uniform external electric field of 0.5 V nm^{-1}.

Table S1. Computed energies and TPA cross sections for *trans*-azobenzene.

Position	Excited state	Energy [eV]		TPA cross section [GM]	
		in vacuum	with Ag(111)	in vacuum	with Ag(111)
C-terminus	S_1	0.97	0.97	0.01	0.01
	S_2	1.93	1.93	1.76	1.62
	S_3	2.18	2.18	2.02	2.06
	S_4	2.20	2.20	1.20	1.26
	S_5	2.25	2.26	0.96	0.85
N-terminus	S_1	0.96	0.96	0.01	0.01
	S_2	1.96	1.95	1.25	1.45
	S_3	2.17	2.17	1.26	1.56
	S_4	2.22	2.22	1.16	1.45
	S_5	2.26	2.26	0.56	0.74

Table S2. Computed energies and TPA cross sections for *cis*-azobenzene.

Position	Excited state	Energy [eV]		TPA cross section [GM]	
		in vacuum	with Ag(111)	in vacuum	with Ag(111)
C-terminus	S_1	1.10	1.12	0.11	0.12
	S_2	2.04	2.02	1.65	3.78
	S_3	2.20	2.18	1.58	2.13
	S_4	2.26	2.26	0.55	0.58
	S_5	2.33	2.31	0.10	0.37
N-terminus	S_1	1.13	1.14	0.11	0.11
	S_2	2.01	2.00	3.00	2.73
	S_3	2.18	2.16	1.05	2.37
	S_4	2.24	2.23	0.91	1.16
	S_5	2.34	2.33	0.21	0.26

Table S3. Calculated dipole moment and transition dipole moment (in a.u.) for ground state and low-lying excited states of *trans*-azobenzene.

trans-azobenzene	conjugated to the C-terminus		conjugated to the N-terminus	
	in vacuum	on Ag(111)	in vacuum	on Ag(111)
‹0|μ|0›	0.680	0.808	0.573	0.695
‹0|μ|1›	0.009	0.012	0.224	0.228
‹0|μ|2›	3.721	3.731	3.530	3.538
‹1|μ|1›	0.143	0.158	0.064	0.084
‹1|μ|2›	0.049	0.041	0.027	0.034
‹2|μ|2›	0.032	0.109	0.061	0.148

Table S4. Calculated dipole moment and transition dipole moment (in a.u.) for ground state and low-lying excited states of *cis*-azobenzene.

cis-azobenzene	conjugated to the C-terminus		conjugated to the N-terminus	
	in vacuum	on Ag(111)	in vacuum	on Ag(111)
‹0|μ|0›	1.413	1.208	2.270	2.532
‹0|μ|1›	0.605	0.621	0.843	0.862
‹0|μ|2›	1.433	1.348	1.886	1.850
‹1|μ|1›	0.536	0.546	0.462	0.454
‹1|μ|2›	0.316	0.427	0.414	0.449
‹2|μ|2›	0.771	1.257	0.676	0.805

Table S5. Calculated two-photon absorption cross-section (in GM) for the most probable conformations of *trans*-azobenzene.

trans-azobenzene	conjugated to the C-terminus		conjugated to the N-terminus	
	in vacuum	on Ag(111)	in vacuum	on Ag(111)
1	2.79	3.21	1.25	4.07
2	4.58	4.24	2.33	2.55
3	3.90	3.34	3.44	5.19
4	1.99	2.62	3.78	3.35
5	9.57	6.69	13.24	12.92
6	4.87	5.22	3.56	3.71
7	4.85	2.33	1.47	1.45
8	8.06	8.62	3.06	3.93
9	12.33	11.53	3.30	3.78
10	5.50	5.36	6.45	7.88
11	8.79	6.56	6.00	6.67
12	8.82	12.20	4.66	5.54
13	14.80	15.87	2.49	3.18
14	2.12	2.47	3.42	5.94
15	5.03	4.06	1.32	1.87
16	3.76	4.37	7.50	7.26

Table S6. Calculated two-photon absorption cross-section (in GM) for the most probable conformations of *cis*-azobenzene.

cis-azobenzene	conjugated to the C-terminus		conjugated to the N-terminus	
	in vacuum	on Ag(111)	in vacuum	on Ag(111)
1	2.37	4.50	2.59	3.62
2	2.96	2.29	5.14	10.70
3	4.81	8.01	5.19	5.44
4	2.91	5.24	7.30	8.65
5	6.26	7.21	17.54	9.38
6	2.19	10.85	6.65	3.14
7	3.50	3.49	1.96	5.48
8	6.84	11.01	1.54	4.58
9	2.83	8.80	4.02	4.17
10	2.71	9.80	2.74	4.63
11	4.51	3.40	1.99	1.83
12	7.29	14.60	1.25	1.69
13	3.63	4.51	2.91	1.22
14	5.04	11.64	5.05	10.65
15	2.98	10.31	5.44	15.34
16	1.75	1.27	4.95	4.90